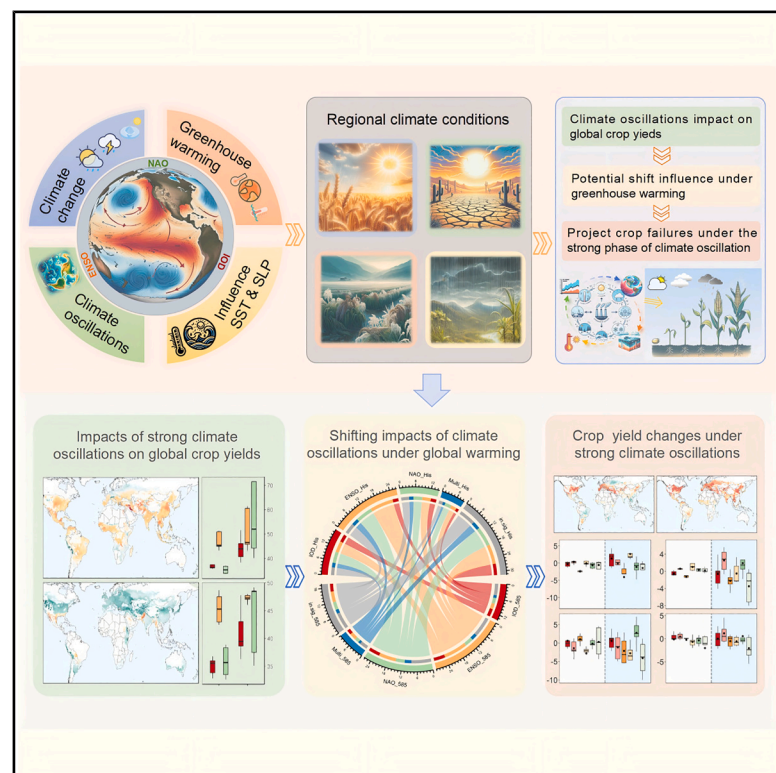


Global warming increases the risk of crop yield failures driven by climate oscillations

Graphical abstract



Authors

Linchao Li, Bin Wang, Puyu Feng, ..., Kadambot H.M. Siddique, Hanqin Tian, Qiang Yu

Correspondence

bin.a.wang@dpi.nsw.gov.au (B.W.),
guijun.yang@163.com (G.Y.),
yuq@nwafu.edu.cn (Q.Y.)

In brief

Global warming tends to amplify the risks of crop failures by intensifying the influence of climate oscillations (e.g., ENSO, IOD, and NAO). Using machine learning and crop-climate model ensembles, this study reveals shifting patterns of climate impacts on crop yields, with increased exposure of cropland to extreme events and rising risks across key agricultural regions. These findings highlight the need to account for dynamic climate variability in strategies to enhance global food-system resilience.

Highlights

- Warming is likely to expose additional cropland to climate oscillation impacts
- The NAO strengthens in the Northern Hemisphere, while the ENSO dominates the South
- Strong negative NAO and El Niño likely increase the risk of simultaneous crop failures

Article

Global warming increases the risk of crop yield failures driven by climate oscillations

Linchao Li,^{1,2,3} Bin Wang,^{4,5,6,21,*} Puyu Feng,⁷ Chaoqun Lu,³ Jonas Jägermeyr,^{8,9,10} Senthold Asseng,¹¹ Jing-Jia Luo,¹² Matthew Tom Harrison,¹³ Qinsi He,¹⁴ Ke Liu,¹³ De Li Liu,^{4,6,15} Yi Li,¹⁶ Hao Feng,² Guijun Yang,^{17,18,*} Chunjiang Zhao,¹⁸ Kadambot H.M. Siddique,¹⁹ Hanqin Tian,²⁰ and Qiang Yu^{2,*}

¹College of Agronomy, Inner Mongolia Agricultural University, Hohhot 010019, China

²State Key Laboratory of Soil Erosion and Dryland Farming on the Loess Plateau, College of Natural Resources and Environment, Northwest A&F University, Yangling 712100, China

³Department of Ecology, Evolution, and Organismal Biology, Iowa State University, Ames, IA, USA

⁴NSW Department of Primary Industries, Wagga Wagga Agricultural Institute, Wagga Wagga, NSW 2650, Australia

⁵Hawkesbury Institute for the Environment, Western Sydney University, Richmond, NSW, Australia

⁶Gulbali Institute for Agriculture, Water and Environment, Charles Sturt University, Wagga Wagga, NSW 2650, Australia

⁷College of Land Science and Technology, China Agricultural University, Beijing 100193, China

⁸NASA Goddard Institute for Space Studies, New York, NY, USA

⁹Columbia University, Center for Climate Systems Research, New York, NY, USA

¹⁰Potsdam Institute for Climate Impacts Research (PIK), Member of the Leibniz Association, Potsdam, Germany

¹¹Technical University of Munich, School of Life Sciences, Department of Life Science Engineering, HEF World Agricultural Systems Center, Freising, Germany

¹²Institute for Climate and Application Research (ICAR), Nanjing University of Information Science and Technology, Nanjing 210044, China

¹³Tasmanian Institute of Agriculture, University of Tasmania, Newnham Drive, Launceston, TAS 7248, Australia

¹⁴School of Life Sciences, Faculty of Science, University of Technology Sydney, PO Box 123, Broadway, NSW 2007, Australia

¹⁵Climate Change Research Centre, University of New South Wales, Sydney, NSW 2052, Australia

¹⁶College of Water Resources and Architectural Engineering, Northwest A&F University, Yangling 712100, China

¹⁷College of Geological Engineering and Geomatics, Chang'an University, Xi'an 710054, China

¹⁸Key Laboratory of Quantitative Remote Sensing in Agriculture of Ministry of Agriculture and Rural Affairs, Information Technology Research Center, Beijing Academy of Agriculture and Forestry Sciences, Beijing 100097, China

¹⁹The UWA Institute of Agriculture and UWA School of Agriculture and Environment, The University of Western Australia, Perth, WA 6001, Australia

²⁰Schiller Institute for Integrated Science and Society, Department of Earth and Environmental Sciences, Boston College, Chestnut Hill, MA 02467, USA

²¹Lead contact

*Correspondence: bin.a.wang@dpi.nsw.gov.au (B.W.), guijun.yang@163.com (G.Y.), yuq@nwfafu.edu.cn (Q.Y.)

<https://doi.org/10.1016/j.oneear.2025.101318>

SCIENCE FOR SOCIETY The stability of the global food system is increasingly challenged as climate extremes driven by natural climate variability become more frequent and more likely to disrupt multiple major crop-producing regions at the same time. The Indian Ocean Dipole (IOD), El Niño-Southern Oscillation (ENSO), and North Atlantic Oscillation (NAO) are the main climate drivers that may influence regional weather conditions and further modulate crop productivity. However, it is still unclear how climate drivers have influenced crop productivity in historical periods and how their impacts may shift in the future. In this study, we integrate artificial intelligence algorithms with a large ensemble of process-based crop and climate models to evaluate the changing impact of climate variability on global crop productivity under greenhouse warming. We find that the NAO is projected to have a stronger influence on crop yields in the Northern Hemisphere and the ENSO increases dominance in the Southern Hemisphere under global warming. These shifting patterns are expected to expose an additional 5.1%–12% of global croplands to climate-oscillation-related disruptions. In addition, strong negative phases of NAO and El Niño events (strong positive phase of ENSO) are likely to cause simultaneous yield losses across multiple key food-producing regions. In contrast, their opposite phases do not demonstrate similar benefits, revealing an asymmetric influence in how these events affect food production and potentially heightening risks to global food security. Understanding these shifting climate signals is critical for building a more resilient food system. Our findings can help farmers and policymakers enhance early-warning systems and develop targeted adaptation strategies to increase food-system resilience and ensure the stability of global food-supply chains.

SUMMARY

Enhancing food-system resilience is critical in the face of increasing climate variability that threatens food security. Large-scale climate oscillations are key drivers of climate conditions that disrupt agricultural productivity. However, how such effects are shifting under greenhouse warming remains unclear. Here, we integrate machine learning with process-based crop models to quantify changes in climate-oscillation-driven yield variability under warming scenarios. We find that climate change increases the dominance of the North Atlantic Oscillation (NAO) in the Northern Hemisphere and the El Niño-Southern Oscillation (ENSO) in the Southern Hemisphere, exposing an additional 5.1%–12% of global croplands to climate oscillation shocks. Negative NAO and El Niño events are projected to cause simultaneous yield losses of 2.0%–8.4% across multiple breadbaskets, while opposite phases provide weaker benefits, indicating asymmetric impacts and greater food security risks. We highlight the importance of incorporating shifting teleconnections into early-warning systems and targeted adaptation strategies to enhance global food-system resilience.

INTRODUCTION

Food production and security have become critical global issues, further complicated by the shift toward globalization and interdependence in contemporary food systems.^{1–3} Climate variability and warming (often leading to extreme drought, flooding, and heat-wave stress) likely impact the food supply and threaten food security and market stability, particularly in regions with limited adaptive capacity.^{4–6} Such risks might be exposed simultaneously to more than one breadbasket, particularly in recent decades,⁷ exacerbating the balance between supply and demand.^{8,9} Given the increasing risk of crop failures and the ever-growing demand for food, identifying the drivers behind simultaneous shocks to food production is essential for developing mitigation strategies toward the zero-hunger target of the Sustainable Development Goals (SDG 2).¹⁰

Large-scale climate drivers, such as the El Niño-Southern Oscillation (ENSO), contain more information compared to local individual climate variables (e.g., temperature or precipitation) due to their interconnected systems that influence weather patterns on a global scale.^{11–14} For instance, an El Niño event typically brings drought to Australia, Indonesia, and neighboring countries.¹⁵ These drivers also influence crop yields through immediate to lagged impacts by modulating regional climate conditions,^{16–18} thus providing a longer lead time and broader outlook than short-term weather predictions.¹⁹ Consequently, there is a need to identify the signals leading to global food production losses in food systems' early warnings.^{20,21} However, in regions like Australia, the dominant climate drivers influencing crop yields, for instance, have shifted from the ENSO to the Indian Ocean Dipole (IOD) over the past century, likely due to the influence of climate warming on regional sea surface temperature (SST) and sea-level pressure (SLP).^{17,22,23} Similarly, the North Atlantic Oscillation (NAO) influences temperature, precipitation, and grain yields in the southeastern United States²⁴ and is expected to have an increasing correlation with precipitation in northern Europe in future scenarios.²⁵ In addition, the ENSO variability is projected to increase under greenhouse warming,^{11,26} potentially increasing the risk of both El Niño and La Niña events. This increase can impact regional dry-wet cycles, leading to more frequent drought and flood events associated with the ENSO due to the greater frequency and intensity of these

events.^{27–29} Evaluating how such shifts in climate drivers will increase the risk of simultaneous shocks to different breadbaskets under greenhouse warming is an important issue for global food security.

Regions negatively affected by climate shocks might find some relief through compensatory approaches from areas experiencing positive impacts through food trade.^{16,30} However, many of these studies rely on traditional linear models to estimate crop yield changes due to climate oscillations,^{16,31} which cannot capture the potential nonlinear responses or the potential shifts with climate change. For instance, extreme rainfall intensifies during El Niño and La Niña, with El Niño events amplifying intensity in East Asia.³² The asymmetric responses of crop yields to climate variations might be underestimated when relying on traditional linear regression analyses. This oversight could inadvertently exacerbate risks to food-supply chains in the face of climate shocks, even with mitigation efforts through food trade. Therefore, quantifying the influence of climate drivers on crop yields under global warming, including both linear and nonlinear relationships, is crucial for farmers and policymakers to develop effective and resilient adaptation strategies.

Wheat (*Triticum* sp. L.), maize (*Zea mays* L.), rice (*Oryza sativa* L.), and soybean (*Glycine max* L. Merr.) are the four major crops globally, providing around two-thirds of human caloric intake.³³ Recent studies have shown that large-scale atmospheric circulations, including the IOD, ENSO, and NAO, significantly affect local climate conditions and crop production.^{16,20,31} However, how climate drivers affect crop yields and their potential shifts under greenhouse gas warming have not yet been comprehensively assessed using model-based analysis.

Here, we employ the latest process-based global gridded crop model intercomparison (GGCMI³⁴) driven by CMIP6 global climate models (GCMs) with a random forest (RF) approach to link climate oscillations (including IOD, ENSO, and NAO) to crop yield. We find that the dominant climate drivers of crop yields are projected to shift under greenhouse warming, with clear changes in regional influence. For instance, the IOD is expected to exert a more independent influence as its historical linkage with the ENSO weakens. Meanwhile, the NAO becomes increasingly dominant in the Northern Hemisphere, and the ENSO strengthens its impact in the Southern Hemisphere. Strong negative NAO (nNAO) phases are projected to elevate

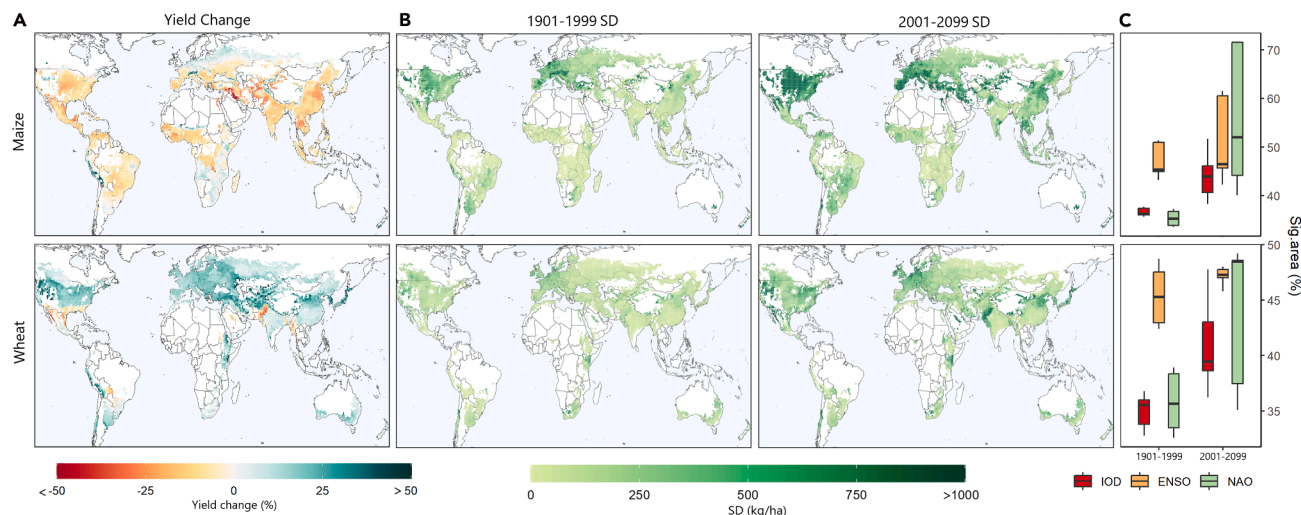


Figure 1. Impact of climate change on crop yield

(A) Multimodel ensemble of crop yield change for wheat and maize spanning historical (1901–1999) and future (2001–2099) periods under SSP585.

(B) Standard deviations (SD) for maize and wheat yield during historical and future under SSP585.

(C) Percentage area significantly influenced by climate drivers (IOD, ENSO, and NAO) for maize and wheat yields based on the five GCMs. Black line denotes median, and the boundaries of each box indicate the 25th and 75th percentiles; whiskers above and below each box mark 10th and 90th percentiles, respectively.

the risk of yield losses across northern breadbaskets, whereas El Niño events increasingly threaten crop production in much of the Southern Hemisphere. However, the modeling framework in this study still has uncertainty, driven by differences among GCMs, GGCMs, and their interactions, with region-specific variation in the dominant sources of uncertainty. This study provides new insights into how climate oscillations modulate crop yields under climate change, identifying key signals that may trigger simultaneous yield losses across global breadbaskets. These findings can support farmers and policymakers in enhancing early-warning systems and developing targeted adaptation strategies to build a more resilient and stable food system.

RESULTS AND DISCUSSION

Changes in crop yield, standard deviations, and areas affected by climate drivers

The ensemble of 12 GGCMs, driven by five different GCMs, revealed distinct impacts of climate change on crop yields. Climate change negatively impacts maize yield and positively impacts wheat yield (Figure 1A), with no significant negative impact on soybean or rice yields in most regions. However, there is a large positive impact on soybean yields in several regions, such as southeast South America, South Africa, and Central Europe (Figure S2). The magnitude of soybean and rice yield changes is not as large as that of wheat and maize, likely due to the large uncertainty in yield projections for soybean and rice.³⁴ In addition, irrigation may help mitigate the impacts of climate change,³⁵ such as increasing the resilience of rice to drought.³⁶ Although CO₂ fertilization can benefit C3 crops like soybean, rice, and wheat, leading to more optimistic projections for these crop yields, the extent of this benefit varies depending on how crop models represent CO₂ fertilization processes.^{34,37} Crop yields are simulated using different crop models driven solely

by climate data, without considering the effects of technological advancements or management practices. This allows us to isolate the impact of climate factors on crop yields. The variability of crop yields, as measured by the standard deviation (SD), is projected to be higher under more severe emissions scenarios (SSP585) across most regions (Figures 1 and S2).

We derived the percentage of areas where crop yields significantly correlate with climate drivers across five GCMs, including the IOD, ENSO, and NAO. We found that for all crop types, areas significantly impacted by drivers show a large increase (Figures 1C and S2C). The impacted maize area increased by 7.7% (from 36.0%–37.4% to 40.6%–46.1%), 3.7% (from 45.1%–50.9% to 45.6%–60.5%), and 18.1% (from 33.8%–36.7% to 44.2%–71.5%) for the IOD, ENSO, and NAO, respectively; wheat areas increased by 5.6% (from 33.8%–36.0% to 38.7%–43.1%), 2.5% (from 42.9%–47.5% to 47.0%–47.8%), and 10.3% (from 33.5%–38.4% to 37.5%–48.6%); soybean areas increased by 9.7% (from 33.8%–37.8% to 40.2%–51.4%), 12.1% (from 45.6%–51.5% to 49.9%–63.6%), and 22.7% (from 34.6%–36.0% to 40.3%–66.2%); and rice areas increased by 2.1% (from 34.2%–48.3% to 36.4%–55.0%), 9.9% (from 57.0%–59.2% to 53.8%–68.5%), and 8.5% (from 36.3%–39.1% to 43.4%–56.2%). These increases suggest that more regions of crop yields are susceptible to those climate drivers in 2001–2099 compared to 1901–1999. Such changes may affect total productivity, with the extent of these variations depending on crop type and regional climate conditions. The future increase in variability compared to the historical period may be due to climate warming influencing the variability of climate oscillations,^{26,38,39} which leads to shifts in regional climate patterns and further affects crop yields, making them more sensitive to these drivers. It is worth noting that there may be some uncertainty due to internal climate variability and differences in how the models represent atmospheric processes.⁴⁰

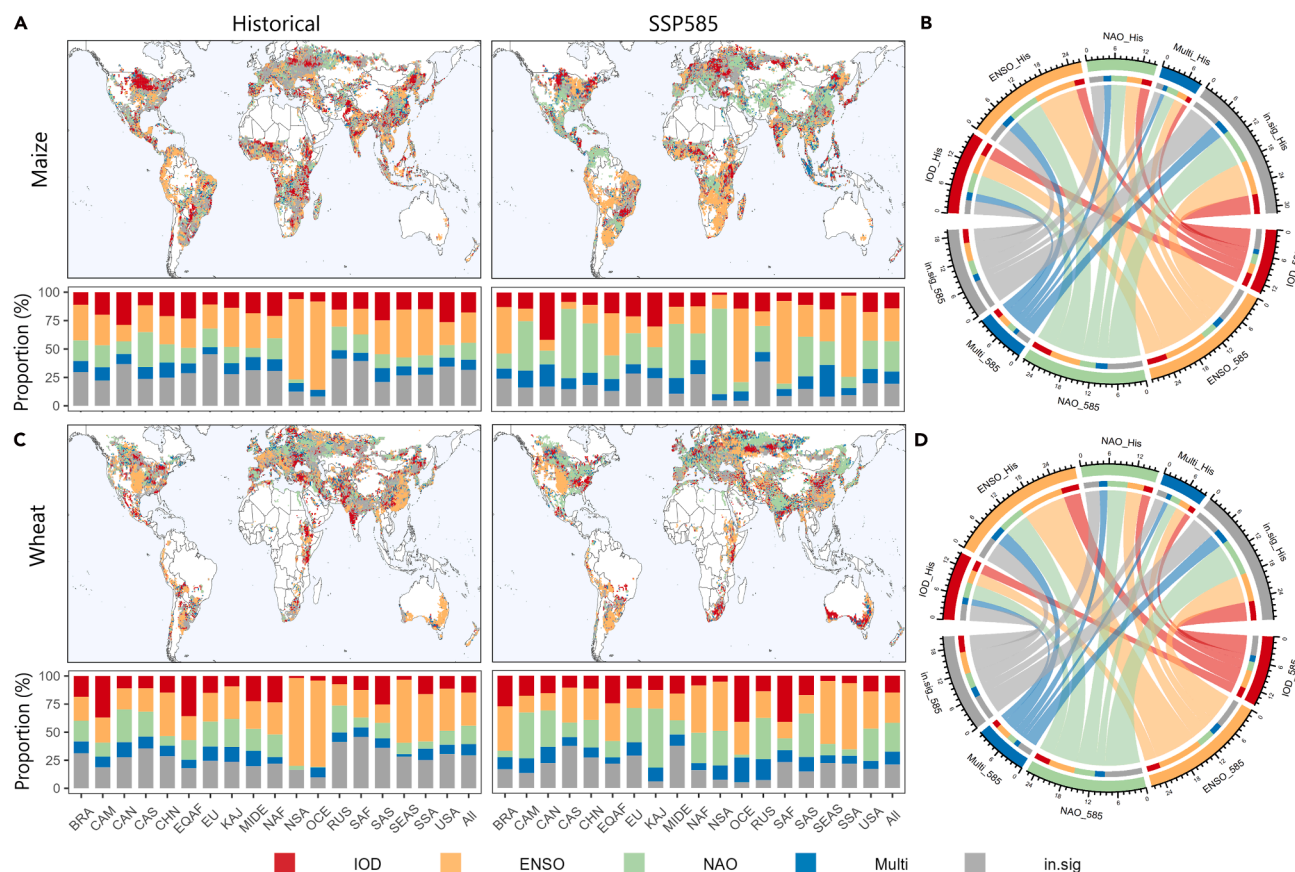


Figure 2. Dominant climatic drivers of global maize and wheat yield identified by the RF model based on GFDL-ESM4

(A and C) (Top) Spatial distribution of dominant factors in historical (1900–1999) and future (2000–2099) periods under SSP585. (Bottom) Proportion of areas by the dominant factor in each sub-region.

(B and D) Chord diagram shows the shift regions in the dominant factor from historical (1900–1999) to future (2000–2099) periods. Multi, the grid in which multiple indices significantly impact crop yield; in.sig, no significant indices. BRA, Brazil; CAM, Central America; CAN, Canada; CAS, Central Asia; CHN, China; EQAF, equatorial Africa; EU, Europe; KAJ, Korea and Japan; MIDE, Mideast; NAF, northern Africa; NSA, northern South America; OCE, Oceania; RUS, Russia; SAF, southern Africa; SAS, South Asia; SEAS, Southeast Asia; SSA, southwest South America; USA, United States of America.

The dominant climate drivers on crop yields

Our results demonstrate the dominant climate drivers in each grid and sub-region (Figure S1) during the two periods (historical and future) under the SSP585 scenario based on GFDL-ESM4 (Figures 2A and 2C). We focus on two 99-year spans (1901–1999 and 2001–2099), since the longer period helps mitigate the effect of internal variability²⁶ and more accurately captures the influence of climate oscillations on crop yields under climate change. Moreover, since we developed the RF model for each grid, a longer period with enough data can ensure the stability of our RF model. The chord diagrams illustrate the shift in dominant climate drivers affecting crop yields from the historical period (1901–1999) to the future period (2001–2099) (Figures 2B and 2D). For example, the link between ENSO_his and IOD_585 indicates that areas where the ENSO was the dominant influence on crop yields during the historical period are projected to shift to being influenced by the IOD in the future. Additionally, the link between in.sig_his and ENSO_585 suggests that regions not significantly affected by climate drivers in the past are expected to be predominantly influenced by the ENSO in the future. The

dominant climate drivers exhibit substantial change between the two periods. For instance, during the historical period, ENSO was the predominant factor influencing crop yields, accounting for 26.1%, 29.2%, 32.5%, and 43.8% of global maize, wheat, soybean, and rice areas, respectively (Figures 2 and S3). During future projections, the NAO is expected to substantially increase dominance of crop yield variance, even if it mainly occurs in the Northern Hemisphere. For example, the NAO's influence on maize yield has increased in northern China (CHN), the Midwest of the United States of America (USA), southern Europe (EU), and the Mideast (MIDE). Conversely, regions dominated by the ENSO, particularly in the Southern Hemisphere, are those such as northeastern Brazil (BRA), southwest South America (SSA), and southern Africa (SAF). Furthermore, the IOD is expected to become the dominant climate driver influencing Australian wheat yield during the 21st century (2001–2099).

Across five GCMs, we find that areas significantly affected by climate variability increase by around 12%, 6.2%, 10%, and 5.1% for maize, wheat, soybean, and rice under future periods compared with historical periods (Figures 2 and S3–S7). Most

GCMs (except MPI-ESM1-2-HR) predict an increased impact of the NAO on crop yields in the Northern Hemisphere, particularly pronounced in the IPSL-CM6A-LR and UKESM1-0-LL models, characterized by high equilibrium climate sensitivity (ECS) and transient climate response (TCR) (Figures S4 and S7). Models with high ECS and TCR often predict stronger and more pronounced global warming with increasing CO₂.^{41,42} The increase in SSTs may influence NAO variability, thereby expanding the areas impacted by climate variability. For instance, under greenhouse warming, SST changes can cause the NAO to shift from a positive to a negative phase in early winter, while reinforcing the nNAO anomaly in late winter.⁴³ Such changes can significantly impact regional climate conditions in the Northern Hemisphere,^{44,45} especially as projected by high ECS and TCR GCMs under high emission scenarios.⁴¹ For example, a strong negative phase of the NAO is often associated with colder, wetter conditions in northern EU, while southern EU may experience warmer and wetter conditions.^{46,47} These climate conditions, driven by an extreme nNAO phase, are likely to impact crop yields. In the Southern Hemisphere, the ENSO is expected to intensify its impact on crop yields in South America and Africa, primarily due to increased ENSO-related hydroclimate variability and the frequency and severity of drought.^{27,48} In Australia, while the ENSO has been the main factor affecting crop yields during historical periods, the IOD is expected to play a more dominant role in the future. This is in line with findings from Feng et al.¹⁷ that global warming increases the frequency of extreme positive IOD (pIOD) events,⁴⁹ and the pIOD phase often brings heat and drought in Australia.^{50,51} Generally, most GCMs project an increase in climate drivers' influence on future crop yields. Only the MRI-ESM2-0 model shows a decrease in areas where climate drivers significantly impact crop yields. This could be attributed to this particular GCM projecting relatively higher crop yields than others,³⁴ suggesting that the climate conditions it predicts may be more favorable for crop growth, with a relatively low frequency of negative impacts from extreme climate oscillation events. Thus, with no significant impact from climate drivers, this model shows relatively low importance as detected by the RF model. However, this does not necessarily mean that the influence of climate modes remains consistently low; it may indicate that the model's projected conditions make crops less sensitive to these drivers, thereby limiting their influence.

Crop yield response to climate drivers

Crop yield perturbations under strong oscillation phases during historical and future periods have been quantified using partial dependence plots (PDPs) based on multimodel ensembles (12 GGCMs and 5 GCMs) under the SSP585 scenario. The spatial patterns of yield change during strong phases of the IOD, ENSO, or NAO can pinpoint global hotspots particularly vulnerable to climate oscillations (Figures 3 and S8–S10). Generally, crop yield changes are expected to become more pronounced, particularly under strong phases of ENSO and NAO, compared with normal phases. For example, strong negative ENSO phases (La Niña) are likely to induce more pronounced losses in maize yields in the USA (0.7%–7.3%), EU (1.9%–4.6%), SSA (1.3%–1.5%), and MIDE (4.6%–8.2%) (Figures 4 and S11), even though the impact may not be statistically significant in some regions. Conversely, it may improve the maize yield in Oceania (OCE)

(3.3%–9.6%), Southeast Asia (SEAS) (1.7%–5%), BRA (1.6%–2.8%), and SAF (2.2%–4.5%) (Figure 4), potentially buffering the negative impact through the food trade. These results are similar to previous studies in most regions,^{19,20,52} though there are some differences in the western part of the EU under both El Niño and La Niña events,¹⁹ as well as different impacts on maize yields in the EU under La Niña events.⁵² These differences may be attributed to variations in data sources, time periods, and methodologies, as our analysis is based on GCM historical data from 1900 to 1999. However, these relationships may not always remain stationary. For example, the ENSO had a limited influence on maize yields in northern South America (NSA) during the historical period, but its impact may increase significantly in the future, leading to substantial yield losses under El Niño events (Figure 4). El Niño could also cause yield losses across multiple regions, with potential reductions of 3.9%–7.7% for maize, 3.1%–8.4% for wheat, 2.8%–6.7% for soybeans, and 2.1%–3.7% for rice. In SEAS, both the ENSO and the IOD will have an increasing influence on maize yields from 2001 to 2099, but the ENSO will remain the dominant driver, with its effects intensifying further (Figure 4). Maize yields in SEAS are likely to decrease during El Niño years, consistent with previous studies,¹⁹ and the ENSO's influence in this region may be further amplified by climate change.^{53,54} Furthermore, global warming is likely to increase the frequency of El Niño events, further amplifying the risk of yield losses.^{55,56}

The strong positive phases of the IOD (pIOD) are projected to negatively affect crop yields in the Southern Hemisphere, particularly wheat, soybean, and rice. Although the spatial patterns of yield changes demonstrate similarity to ENSO-induced yield change during the historical period (Figures 3 and S8–S10), they exhibit variation under future climate changes (Figures 3 and S8–S10). As El Niño develops, the associated weakening of the Walker Circulation can reduce upwelling in the eastern Indian Ocean, leading to warmer SSTs in the western part and cooler conditions in the eastern part.^{57,58} Consequently, El Niño events and pIOD have often been interconnected, likely exerting similar impact patterns on crops during historical periods (Figure 3). However, their influence differs significantly in future periods (Figure 3), possibly due to a weakening ENSO-IOD connection.⁵⁹ For a typical instance, in 2019, a very weak El Niño coupled with a strong pIOD led to dry and hot weather in eastern Australia, culminating in devastating bushfires.^{60,61} This indicates that in Australia, the impact of pIOD is not always similar to that of El Niño. Therefore, under climate change, the impacts of the ENSO and IOD on crop yields may increasingly diverge, as seen in the different yield changes under extreme IOD and ENSO events for maize (Figures 3 and 4). Furthermore, although the IOD-induced yield losses are less than those caused by the ENSO, extreme IOD events are projected to increase under global warming,⁴⁹ indicating a still large impact.

In historical periods, the NAO has been linked to yield losses in the USA, Russia (RUS), and EU during extreme nNAO for maize, wheat, and soybean, aligning with findings from previous studies.^{16,20,52} In future periods, climate change is expected to amplify the NAO's influence on crop yields in the Northern Hemisphere (Figure 3). We show that nNAO increases the risk of simultaneous crop yield shocks across different breadbaskets (Figures 3 and S8–S11) during the future period. For instance,

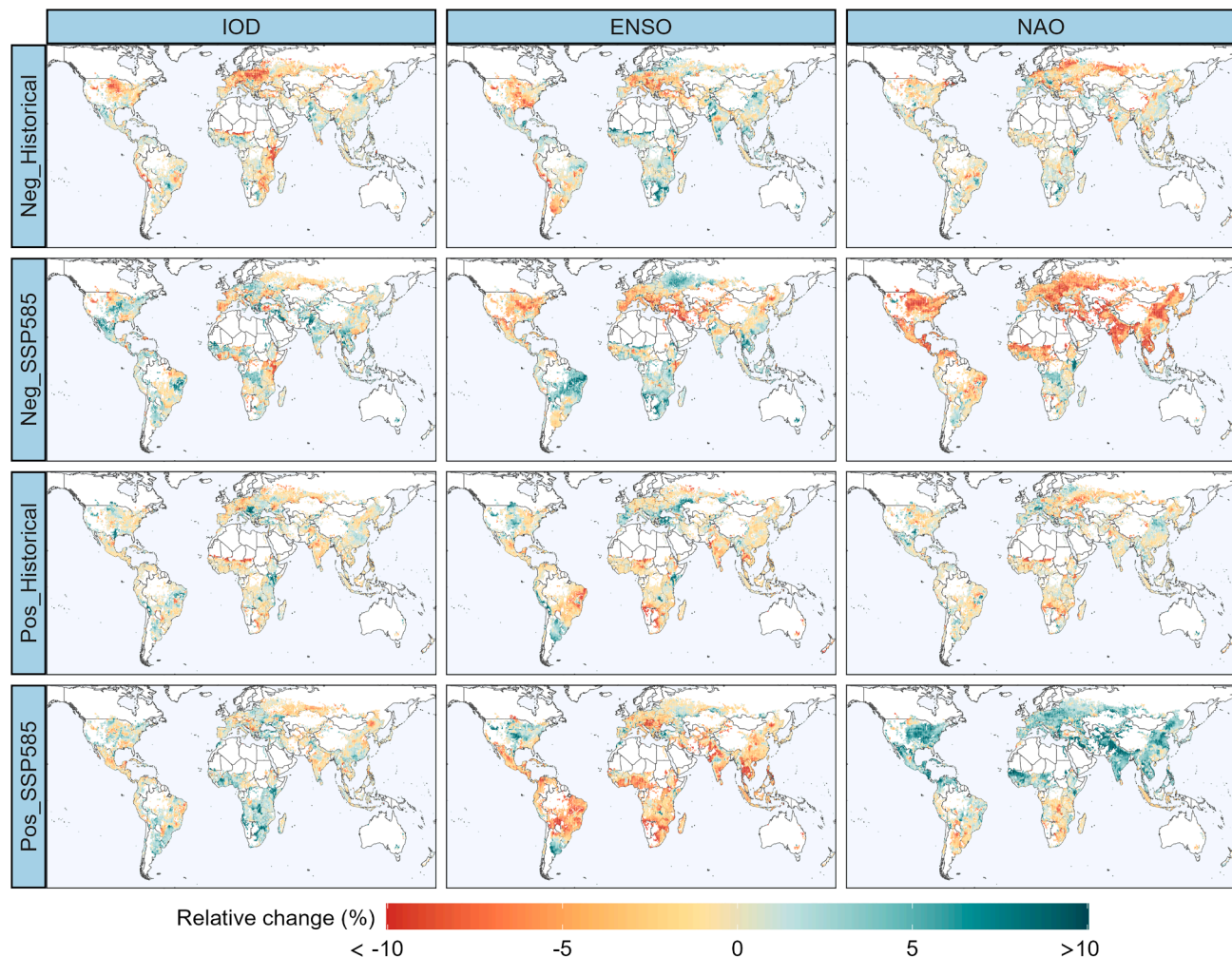


Figure 3. Maize yield changes under strong phases of the IOD, ENSO and NAO

Maize yield changes were estimated using partial dependence plots from a random forest model, based on a multimodel ensemble (12 GCMs and 5 GCMs) under the SSP585 scenario, during both historical (1901–1999) and future (2001–2099) periods. Neg_Historical represents the crop yield change during a strong negative phase (10th percentile) compared with a normal phase (50th percentile) in the historical period. Neg_SSP585 denotes the crop yield change during a strong negative phase (10th percentile) compared with a normal phase (50th percentile) in the future period under SSP585. Pos_Historical represents the crop yield change during a strong positive phase (90th percentile) compared with a normal phase (50th percentile) in the historical period. Pos_SSP585 represents the crop yield change during a strong positive phase (90th percentile) compared with a normal phase (50th percentile) in the future period under SSP585. The other crops (wheat, soybean, and rice) are shown in [Figures S8–S11](#).

extreme nNAO events could decrease maize production by 0.01%–13.2% in the USA, 0.4%–7.5% in EU, 0.18%–15.2% in Central Asia (CAS), 0.01%–11.4% in CHN, and 2.8%–7.7% in South Asia (SAS) ([Figure 4](#)). Generally, different crops in the Northern Hemisphere are also expected to experience different degrees of decline under extreme nNAO events ([Figures S11–S13](#)), with potential decreases of 4.1%–6.9% for maize, 2.8%–6.9% for wheat, 2.7%–6.3% for soybean, and 2%–9.9% for rice across different affected regions. In regions such as CAS, northern Africa (NAF), and CHN, where the NAO historically had little impact on yields, its influence is expected to increase. This shift is perhaps because greenhouse warming amplifies ocean heat transport and alters atmospheric circulation, thereby increasing the NAO's dominance in these regions.⁴⁴ Several studies also highlight the relationship between the NAO and

extreme climate events in the Northern Hemisphere.^{25,62,63} Despite potential yield benefits during positive phases of NAO (pNAO), yield losses may be outweighed during nNAO phases ([Figures 4 and S11–S13](#)). Furthermore, our study reveals significant uncertainties in NAO-induced yield changes due to differences in physical processes among GCMs.⁶⁴

Our study highlights the asymmetric effects of climate drivers on crop yield, indicating net losses during intense climate oscillation phases. For example, El Niño positively affects one of the world's major food baskets in southern South America (such as southern Brazil, Argentina, Uruguay, and Paraguay) while negatively impacting the northern part of South America. La Niña generally has the opposite effect ([Figures 3 and S8–S10](#)). However, the negative impacts from climate oscillations are increasing and are not fully offset by the positive effects

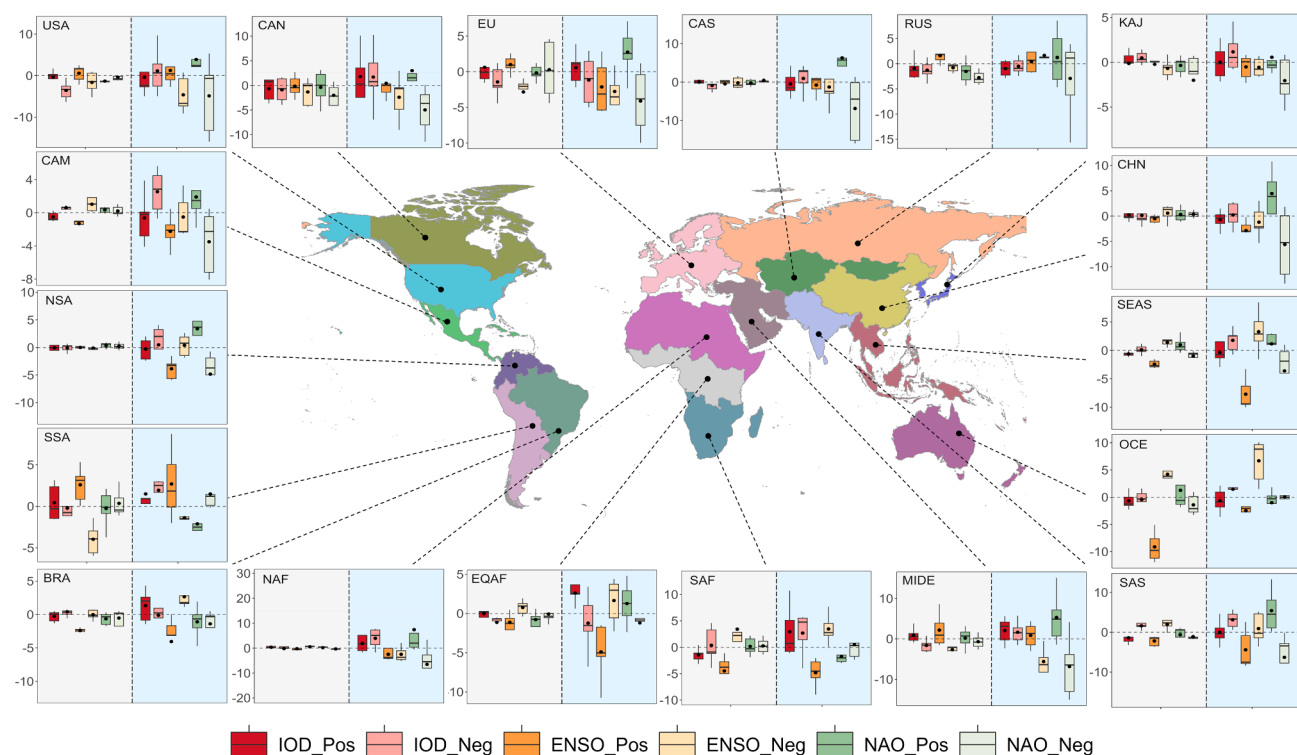


Figure 4. Regional maize yield changes (%) under strong phases of climate drivers

Boxplots denote maize production simulated by 12 GGCMs and 5 GCMs. The black line denotes the median, the boundaries of each box indicate the 25th and 75th percentiles, and whiskers above and below each box mark the 10th and 90th percentiles, respectively. Pos, the maize production change during a strong positive phase (90th percentile) compared with a normal phase (50th percentile) in the historical period; Neg, the crop yield change during a strong negative phase (10th percentile) compared with a normal phase (50th percentile) in the historical period. BRA, Brazil; CAM, Central America; CAN, Canada; CAS, Central Asia; CHN, China; EQAF, equatorial Africa; EU, Europe; KAJ, Korea and Japan; MIDE, Mideast; NAF, northern Africa; NSA, northern South America; OCE, Oceania; RUS, Russia; SAF, southern Africa; SAS, South Asia; SEAS, Southeast Asia; SSA, southwest South America; USA, United States of America.

associated with climate change. Recent trends also suggest prolonged La Niña events,^{65,66} which increase the risk of droughts and yield losses in southern South America. Moreover, extreme flood events are associated with the ENSO, such as the severe floods in southern Brazil in 2024 during an El Niño year⁶⁷ and flooding in Colombia during a La Niña year,⁶⁸ which have the potential to reduce crop yields.^{6,69,70} However, current crop models have not fully captured these extreme wet conditions,^{6,71} resulting in overestimating yields under extreme wet conditions induced by climate oscillation. Consequently, this may lead to underestimating the risks of crop yield losses during extreme wet years driven by climate oscillations. Such risks could pose additional challenges to food security and hinder the achievement of SDG 2.

We employ the RF model to quantify crop yield changes during strong climate oscillation phases, effectively capturing potential nonlinear relationships. However, this method may only partially demonstrate the spatial patterns of crop yield responses during transitional periods between the positive and the negative strong phases of the oscillations. Thus, we used a multivariate dynamic linear model (DLM) to analyze the sensitivity of crop yields to climate drivers. The results show that the sensitivity of crop yield to climate drivers is increasing in most regions (Figures S11 and S12), especially in those with a higher SD of crop yield (see

supplemental methods). Overall, this study identified two climate signals likely to amplify the risk of simultaneous crop production failure: nNAO and El Niño.

Uncertainty analysis

The impact of climate drivers on crop yields under climate change was evaluated based on a large ensemble of process-based crop and climate models. However, we understand that there is a large uncertainty in such analysis sourced from GGCM, SSP, and GCM, which still needs to be fully quantified. The studies for analyzing sources of uncertainty in crop yield change projections have been well documented from site to global scales,^{37,71–75} and a package of approaches in constraining uncertainty has been developed through different pathways.^{76,77} However, in estimating the impacts of climate drivers, the sources of uncertainty may vary from those in previous studies due to differences in modeling approaches. Identifying the sources of uncertainty in the impact of climate drivers on crop yields is essential for better understanding climate shock assessments on breadbaskets under greenhouse warming. Furthermore, it can provide new insights and pathways to reduce the overall uncertainty in climate change impact studies and improve the precision and reliability of seasonal crop yield forecasts.

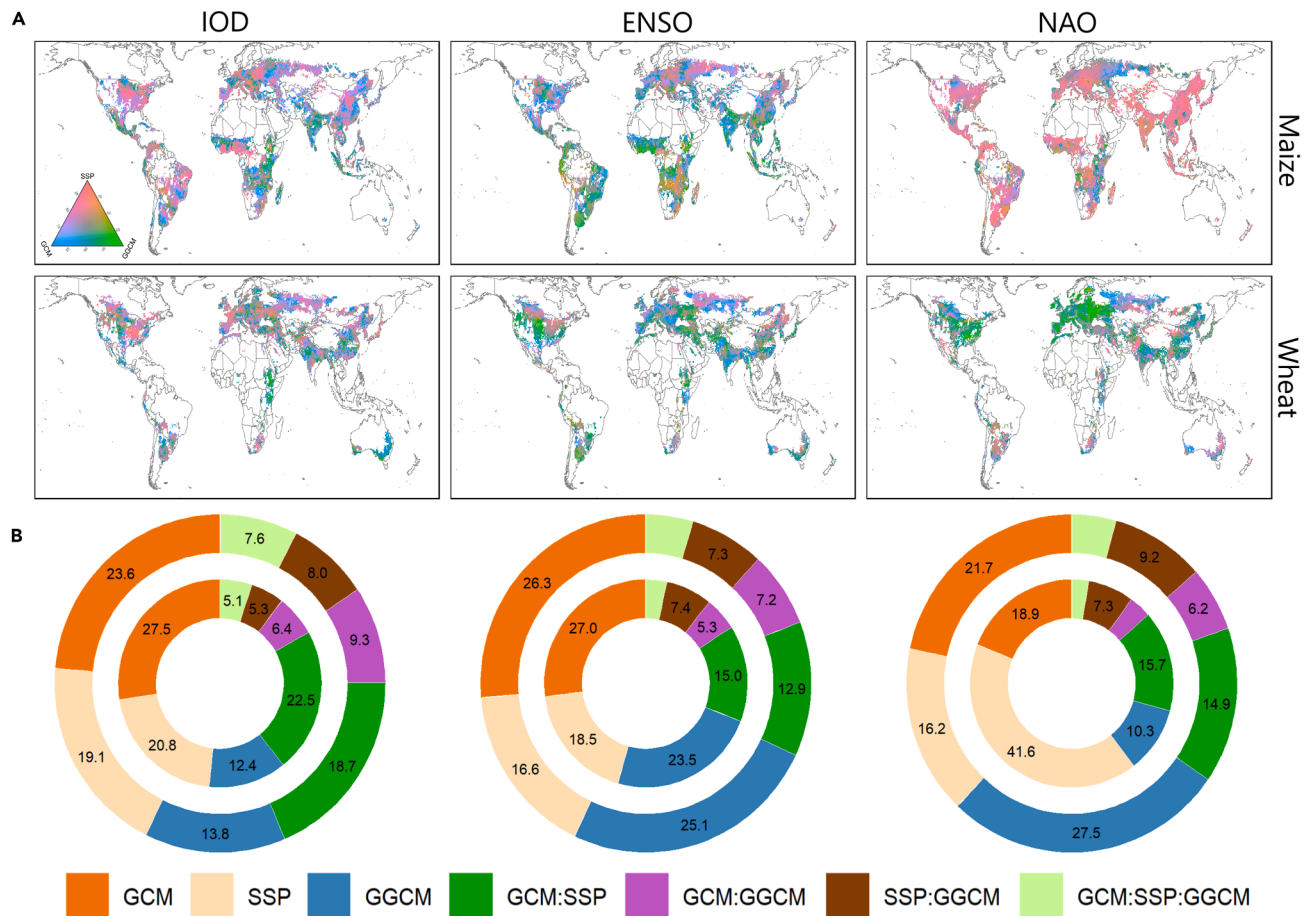


Figure 5. Source of uncertainty in the sensitivity of maize and wheat yields to climate drivers (IOD, ENSO, and NAO) under climate change
(A) Spatial pattern illustrating the fraction of uncertainty attributable to GCM, GGCM, and SSP.
(B) Spatially averaged contributions from each source of uncertainty, along with their pairwise and triple interactions, relative to the total ensemble uncertainty. The inner circle represents the uncertainty share for maize and the outer ring represents the uncertainty share for wheat.

In this study, we employed an analysis of variation (ANOVA) approach to quantify the spatial patterns of relative contributions from various uncertainty sources (see [supplemental methods](#)). The results revealed that uncertainties from GCMs and SSPs are larger than those induced by GGCMs. This raises the question of why the dominant source of uncertainty is the GCM and SSP rather than the crop model compared with previous studies.^{34,37,78} A potential explanation is the differing modeling chains employed. Crop yield projections rely on crop models driven by a GCM. Because of the complexity of biological processes and the interactions between crop growth and environmental variables, the crop model may induce more uncertainties.^{73,74} However, in assessing the impact of climate drivers on crop yield, the representation of these climate drivers (e.g., IOD, ENSO, and NAO) in different GCMs becomes important and may have different impacts on local weather conditions. Consequently, the complex simulations provided by GCMs can bring additional uncertainties.^{53,64,79} Furthermore, we found that regions where uncertainties are mainly sourced from the GCM are more likely vulnerable to climate drivers ([Figures 5 and S18](#)). This is mainly because such regions are susceptible to climate variability and extreme events induced by climate drivers.

For instance, in the Australian wheat belt, GCM is the dominant source of uncertainty in analyzing the IOD's impact on crop yields ([Figure S18](#)), likely because the wheat yields in the Mediterranean climate are more likely affected by natural variability,⁷³ and the IOD also shows an increasing dominance in influencing the Australian wheat belt.¹⁷ Such methods provide new insights into the impact of climate variability drivers on crop yields, allowing us to identify regions at high risk of being impacted by climate oscillations.

Implications for global food security

Our study has wide-ranging implications for global food security. Climate teleconnections significantly influence regional climate conditions, which in turn can impact local food production,¹⁹ ecosystems,^{14,80} and socioeconomic factors.^{81,82} The sensitivity of these connections is more significant under future climate change.²⁷ Given that climate drivers such as the ENSO influence various climate factors, they offer more harmonious insight compared with singular climatic indicators (e.g., temperature, radiation, or precipitation).^{13,15} In addition, many studies still mostly focus on the impact of the ENSO,^{21,27} which potentially overlooks crucial information and results in insufficient

preparedness for adverse agricultural climate conditions. Our study, integrating machine learning techniques with multimodel ensembles, provides a comprehensive insight into how historical teleconnections of climate drivers have influenced global crop production and anticipates their evolution in a future warmer climate. For instance, the NAO increases dominance in the Northern Hemisphere (Figure 2), and the IOD has a more independent effect on crop yield in OCE under future warming (Figures 3 and 4). Here, we identify climate signals that could lead to high risks of simultaneous shocks across multiple breadbaskets. As the food system becomes increasingly globalized, localized shocks can potentially affect vulnerable people in geographically distinct zones through the food trade network.^{83,84}

Our results highlight the importance of considering climate oscillations in proactively enhancing the resilience of food systems. We identified potential shifts in the impact of climate oscillations due to global warming, a trend that warrants significant attention given the ongoing rise in global temperatures. For example, we found that the IOD will increasingly dominate the influence on Australian wheat yields compared to the historical period, consistent with Feng et al.¹⁷ This highlights the need to dynamically consider dominant climate drivers to more accurately project crop yield changes resulting from climate oscillation shocks, especially under warming conditions. Thus, our study suggests improving the robustness of crop yield forecasting systems by accounting for the potential shift in dominant climate drivers. Robust projections can help policymakers and stakeholders prepare for potential coming risks by building more resilient food systems that can better withstand future climate shocks.⁸⁵ For instance, investments in infrastructure to enhance resilience to projected changes, improvements in food stock technology and capacity to buffer potential shocks, and the refinement of trade policies based on accurate climate oscillation signals will be crucial in mitigating the negative impacts of future climate variability on food production.^{30,86–88} We also found that in regions such as Korea and Japan (KAJ), northern CHN, and Central America (CAM), crop yields for maize, wheat, and rice are projected to decrease under both El Niño and La Niña events. Regarding the NAO, our findings indicate that the NAO increases crop yield losses across most of the Northern Hemisphere, with these losses outweighing any yield benefits observed under pNAO phases. These nonlinear and asymmetric effects add additional risks under climate change, which are potentially underestimated by simple linear models.^{65,82} This may exacerbate the stability of food-supply chains and pose additional challenges to global food security. More importantly, countries experience and respond to food market volatility differently, depending on their exposure to market shocks and their capacity to adapt and recover.⁸⁶ For example, limited supply flexibility and slow dietary changes in developing countries increase vulnerability to food shortages and price spikes.⁸⁹ Therefore, it is essential to implement a tailored strategy that accounts for climate teleconnections, particularly in countries or regions with low resilience to climate change.

Limitations and future framework

There are some limitations in this study. First, although our analysis used multimodel ensembles, it still has large uncertainties (supplemental methods). The projections of crop yield changes

are subject to uncertainties arising from model structure, parameters, GCMs, soil data, and other factors, which pose challenges to accurate predictions.^{34,90} The ENSO, IOD, and NAO projections are also highly uncertain due to complex and multidirectional feedback, internal variability, and nonlinear dynamics.^{91,92} For instance, small perturbations in initial conditions can lead to large variability, highlighting the complexity and challenges in projecting ENSO.⁹² Similarly, NAO projections are uncertain due to the representation of physical processes and internal variability.⁶⁴ Moreover, projections of climate drivers are further complicated by anthropogenic influences, adding additional uncertainty to climate oscillation projections.^{64,93} However, we did not constrain the uncertainties associated with climate drivers or crop yield projections in this study. Several methods could address these limitations. For example, Wang et al.⁷⁶ constrain the gridded global crop models' response to warmer temperatures based on field data with an emergent-constraint method. Projections of climate drivers based on GCMs often exhibit large biases. Tang et al.⁹⁴ identified systematic biases in 13 models simulating historical climate and presented more reliable extreme El Niño frequency projections by removing such biases. Therefore, applying systematic bias corrections in climate models may help provide more robust projections. In addition, since climate drivers have different patterns in disrupting the global crop yield, integrating empirical crop yield responses to climate drivers to better harmonize the crop and climate could be a useful approach to reduce the uncertainty in crop yield predictions. Second, while the study highlights the importance of understanding the impacts of climate drivers (ENSO, IOD, and NAO) on food baskets, future research could explore dynamic farming practices and adaptation strategies to enhance resilience.¹⁷ Approaches such as adaptation of crop calendars,⁹⁵ changes in irrigation,³⁵ and optimization of fertilizer use,⁹⁶ which could buffer the negative shock of strong climate oscillations, could be considered. These adaptations could influence the relationship between climate drivers and crop yield. Future work will incorporate different climate change adaptation strategies to meet more severe and complete knowledge needs. Third, the study primarily focuses on the relationship between climate drivers and crop yields without delving into potential trade policy strategies. Understanding how climate oscillations could impact international food trade and exploring potential trade policy responses could significantly contribute to enhancing food security.⁹⁷ Previous studies mainly explored the nexus between climate change and international trade^{30,98,99} rather than linking climate oscillations to international trade. Understanding how climate oscillations potentially influence food trade could provide valuable insights for enhancing food security under climate change.

METHODS

Global crop yield simulation

Here, we leverage global process-based crop model simulations from AgMIP's GGCMI project phase 3.³⁴ We select 12 GGCMI (ACEA, CROVER, CYGMA1p74, DSSAT-Pythia, EPIC-IIASA, ISAM, LandscapeDNDC, LPJmL, pDSSAT, PEPIC, PROMET, and SIMPLACE-LINTUL5) to evaluate historical and future crop yields. The crop models are forced by five bias-adjusted and

downscaled daily CMIP6 GCMs (GFDL-ESM4, IPSL-CM6A-LR, MPI-ESM1-2-HR, MRI-ESM2-0, and UKESM10-LL) from the ISIMIP framework. We considered two climate change scenarios in this study, SSP126 and SSP585, a high-mitigation and a high-emissions scenario. We focused on four major crops, including wheat, maize, rice, and soybeans, each under both rainfed and fully irrigated conditions. Irrigation is modeled by keeping soil moisture at field capacity to assess yield responses without water limits. We use constant crop areas in this simulation. Results are aggregated based on the current cropland distribution at a $0.5^\circ \times 0.5^\circ$ global grid.¹⁰⁰ For more information on the modeling protocol, harmonization, and performance of the crop models, see Jägermeyr et al.³⁴ Several studies have employed crop models like APSIM and LPJm1 to analyze the impact of climate drivers on crop yields.^{16,17} However, relying on a single model could lead to large uncertainties in crop yield simulations due to model structure and parameter variations.³⁷ In our study, we utilize an ensemble of 12 GCMs for a more rigorous and robust analysis.

Large-scale climate drivers

In this study, we employed three specific oscillation indices to capture the variability of key climate mode: the Dipole Mode Index (DMI) for the IOD, the Niño3.4 index for the ENSO, and the NAO index for the NAO itself. These three indices (ENSO, IOD, and NAO) were selected due to their known variability and potential impacts on global climate patterns, including extreme weather events that can significantly influence crop yields.³¹ Furthermore, these climate oscillations are known to have a significant impact on crop yields worldwide due to their influence on regional weather patterns and have been extensively used in previous studies to represent climate variability.^{16,20,31,52} Although other oscillation indices, such as the Pacific Decadal Oscillation (PDO), Atlantic Multidecadal Oscillation (AMO), and Arctic Oscillation (AO), also likely impact global climate patterns and extreme weather events, potentially influencing crop yields,^{101,102} our study primarily focuses on interannual variability. The decadal nature of such oscillations, while important, was likely not suitable for this study due to its longer-term nature. Thus, the ENSO, IOD, and NAO are more directly relevant to and suitable for this study.

The Niño3.4 index was calculated by area-averaged SST within the Niño3.4 region (170°W – 120°W and 5°S – 5°N).¹⁰³ The ENSO is one of the major climate drivers strongly associated with global climate conditions.¹⁰⁴ Although the ENSO is formed in the tropical Pacific, the impact reach is global, including the social economy,^{12,81} ecosystems,⁵³ and food production.¹⁹ Given that the ENSO has been shown to strongly affect global crop production,^{19,105,106} it is suitable to decouple food production from the ENSO under climate change. In this study, we used the Niño3.4 index to represent the ENSO. Many GCMs project stronger ENSO variability under greenhouse warming.^{11,26} Four of the five GCMs used in our study also show an increase in ENSO variance, excepting UKESM1-0-LL, which projects a decrease. This discrepancy highlights intermodel uncertainties, likely due to differences in internal feedback and dynamical processes, which may influence projected crop yield responses under future climate scenarios.

The IOD is expressed by an anomalous SST gradient among the western equatorial Indian Ocean (50°E – 70°E and 10°S –

10°N) and the southeastern equatorial Indian Ocean (90°E – 110°E and 10°S – 0°N).¹⁰⁷ The IOD is also a major climate driver that influences the risk of extreme precipitation and drought.¹⁰⁸ The strong IOD phases independently affect the regional climate condition, further influencing land photosynthesis⁵¹ and crop yields.¹⁷ For instance, pIOD-induced hot-dry weather largely contributed to bushfires during 2019–2020 in Australia.⁶¹

We use the NAO defined as the difference in area-averaged SLP between a southern region (90°W – 60°E and 20°N – 55°N) and a northern region (90°W – 60°E and 55°N – 90°N) in the North Atlantic, following previous studies.^{62,64} This method is less sensitive to differences in centers of action among observations and models than the station-based index.^{62,64} This study included the NAO as it particularly affects the climate in the Northern Hemisphere, such as EU and North America, which is often associated with extreme events (hot or wet), snow cover, and wind.¹⁰⁹ Thus, the NAO further influences crop growth and yields, especially in the Northern Hemisphere.^{31,52}

We used the five CMIP6 GCMs to project the variability of such three climate driver indices under SSP126 and SSP585. In this study, the strong oscillation phases were assumed when they were higher (or lower) than the 90th (10th) percentile during the two periods (historical, 1901–1999, and future, 2001–2099). To demonstrate the climate driver indices' impact on crop yields in different sub-regions, we used 18 regions based on Tian et al.,¹¹⁰ including BRA, CAM, CAN (Canada), CAS, CHN, EQAF (equatorial Africa), EU, KAJ, MIDE, NAF, NSA, OCE, RUS, SAF, SAS, SEAS, SSA, and the USA (Figure S1). Although these regions may not be fully applicable across all climate drivers, defining regions based on a country list makes it easier to connect our findings with region-specific implications and policy considerations.

Identifying the dominant climate drivers

We employed the RF model with three climate drivers (IOD, ENSO, and NAO) to identify the dominant climate drivers of different crop yields. The RF model is a popular algorithm based on multiple regression trees, which can be used to analyze the nonlinear response between different factors. In this study, the detrended growing season climate drivers (from five GCMs) and crop yields (12 GCMs ensemble) were used in the RF model. The relative importance can be calculated using an out-of-bag (OOB) validation procedure from the fitted RF model. As there are large biases among GCMs in climate driver projections^{64,79} and the potential offsetting of strong phases of climate drivers in different models, we present the shifting dominant factors using individual GCMs rather than using a multimodel ensemble. We normalized the importance value to sum to 100% for five GCMs under SSP585. The factor with maximum importance value was identified as a dominant factor in influencing crop yields. We identified the regions as having more than one dominant climate driver when the SD (between ENSO, NAO, and IOD) was lower than 10%. The importance value and significance level were calculated by the “rfPermute” package in R.¹¹¹ In this study, we identified the significant areas where the p value is lower than 0.33. Recently, there has been guidance that utilizes the terms “very unlikely,” “unlikely,” and “likely” for the 0%–10%, 0%–33%, and 66%–100% probability of the likelihood of the outcome, respectively.^{53,112} Our results

suggest that it is unlikely for strong oscillation phases to exhibit no Granger causality on crop yields, leading us to posit a causal linkage between climatic oscillations and agricultural productivity in the identified regions.

Quantifying the climate drivers' impacts on crop yields

The response functions of climate drivers and crop yields were demonstrated by calculating partial dependence using the RF model. The partial dependence plot can reveal whether the relationships between climate drivers and crop yields are linear, nonlinear, or more complex.¹¹³ Here, we built an RF model for each grid using the “pdp” R package. We quantified the crop yield change between strong oscillation phases (negative, 10th; positive, 90th) and neutral phases (50th) based on the partial dependence functions. It is worth noting that we used a multi-model ensemble to evaluate yield losses under the strong phases of climate drivers. In this condition, the signal of the climate oscillations is not offset, as the focus is specifically on yield changes during these conditions.

Map spatial smoothing processing

The map spatial smoothing processing consists of two main steps: first, we resampled it to a resolution five times finer; then, a 5×5 grid cell focal mean window aggregation was applied to smooth the map. It's important to note that this smoothing is exclusively for visualization, and all analyses were conducted using the original, raw data.

RESOURCE AVAILABILITY

Lead contact

Requests for further information and resources should be directed to and will be fulfilled by the lead contact, Bin Wang (bin.a.wang@dpi.nsw.gov.au).

Materials availability

This study did not generate new unique materials.

Data and code availability

All data used in this study are publicly available and cited in the article or supplemental information. CMIP6 climate data can be accessed via the Earth System Grid Federation (<https://esgf-node.llnl.gov/projects/cmip6/>), and model input data are available from the ISIMIP repository (<https://www.isimip.org/>). The GGCM crop calendar is available at <https://doi.org/10.5281/zenodo.5062513> and fertilizer input data at <https://doi.org/10.5281/zenodo.4954582>. The RF modeling was performed using the “randomForest” package in R 4.1.1 (<https://cran.r-project.org/web/packages/randomForest/>). Additional information, code, and resources are available from the lead contact upon reasonable request.

ACKNOWLEDGMENTS

This study was supported by the National Key Research and Development Program of China (2023YFD2000100) and the Natural Science Foundation of China (42171303). It was also supported by the collaboration project jointly founded by the NSFC (grant no. 41961124006) and the NSF (grant no. 1903722) for Innovations at the Nexus of Food, Energy, and Water Systems (INFEWS: US–China). We acknowledge the Agricultural Intercomparison and Improvement Project (AgMIP), the Inter-Sectoral Impact Model Intercomparison Project (ISIMIP), and the contributing modelers for making crop model simulations available. We acknowledge the World Climate Research Program, which, through its Working Group on Coupled Modeling, coordinated and promoted CMIP6. We thank the climate modeling groups for producing and making available their model output, the Earth System Grid Federation (ESGF) for archiving the data and providing access, and the multiple funding agencies

that support CMIP6 and ESGF. We are also grateful to the anonymous reviewers and editors for their valuable comments and recommendations.

AUTHOR CONTRIBUTIONS

Conceptualization, L.L., B.W., and Q.Y.; methodology, L.L., C.L., S.A., and J. J.; software, K.L., P.F., J.J., and S.A.; validation, K.L., J.-J.L., Q.H., and J.J.; formal analysis, L.L., P.F., and J.J.; investigation, L.L., H.F., Y.L., and P.F.; resources, D.L.L., C.Z., and G.Y.; data curation, P.F., K.L., and J.J.; writing – original draft, L.L., B.W., and P.F.; writing – review & editing, B.W., G.Y., H. T., S.A., and K.H.M.S.; supervision, G.Y., H.T., and Q.Y.; project administration, C.Z. and Q.Y.; funding acquisition, Q.Y. and G.Y.

DECLARATION OF INTERESTS

The authors declare no competing interests.

SUPPLEMENTAL INFORMATION

Supplemental information can be found online at <https://doi.org/10.1016/j.oneear.2025.101318>.

Received: June 14, 2024

Revised: October 24, 2024

Accepted: April 29, 2025

Published: May 23, 2025

REFERENCES

1. Lam, H.-M., Remais, J., Fung, M.-C., Xu, L., and Sun, S.S.-M. (2013). Food supply and food safety issues in China. *Lancet* 381, 2044–2053. [https://doi.org/10.1016/s0140-6736\(13\)60776-x](https://doi.org/10.1016/s0140-6736(13)60776-x).
2. Wheeler, T., and von Braun, J. (2013). Climate change impacts on global food security. *Science* 341, 508–513.
3. Puma, M.J., Bose, S., Chon, S.Y., and Cook, B.I. (2015). Assessing the evolving fragility of the global food system. *Environ. Res. Lett.* 10, 024007. <https://doi.org/10.1088/1748-9326/10/2/024007>.
4. Gohar, A.A., and Cashman, A. (2016). A methodology to assess the impact of climate variability and change on water resources, food security and economic welfare. *Agric. Syst.* 147, 51–64. <https://doi.org/10.1016/j.agry.2016.05.008>.
5. Ray, D.K., Gerber, J.S., MacDonald, G.K., and West, P.C. (2015). Climate variation explains a third of global crop yield variability. *Nat. Commun.* 6, 5989. <https://doi.org/10.1038/ncomms6989>.
6. Liu, K., Harrison, M.T., Yan, H., Liu, D.L., Meinke, H., Hoogenboom, G., Wang, B., Peng, B., Guan, K., Jaegermeyr, J., et al. (2023). Silver lining to a climate crisis in multiple prospects for alleviating crop waterlogging under future climates. *Nat. Commun.* 14, 765. <https://doi.org/10.1038/s41467-023-36129-4>.
7. Gaupp, F., Hall, J., Hochrainer-Stigler, S., and Dadson, S. (2019). Changing risks of simultaneous global breadbasket failure. *Nat. Clim. Chang.* 10, 54–57. <https://doi.org/10.1038/s41558-019-0600-z>.
8. Hasegawa, T., Fujimori, S., Havlík, P., Valin, H., Bodirsky, B.L., Doelman, J.C., Fellmann, T., Kyle, P., Koopman, J.F.L., Lotze-Campen, H., et al. (2018). Risk of increased food insecurity under stringent global climate change mitigation policy. *Nat. Clim. Chang.* 8, 699–703. <https://doi.org/10.1038/s41558-018-0230-x>.
9. Martini, G., Bracci, A., Riches, L., Jaiswal, S., Corea, M., Rivers, J., Husain, A., and Omodei, E. (2022). Machine learning can guide food security efforts when primary data are not available. *Nat. Food* 3, 716–728. <https://doi.org/10.1038/s43016-022-00587-8>.
10. United Nation (2015). Transforming our world: the 2030 Agenda for Sustainable Development.
11. Cai, W., Santoso, A., Collins, M., Dewitte, B., Karamperidou, C., Kug, J.-S., Lengaigne, M., McPhaden, M.J., Stuecker, M.F., Taschetto, A.S., et al. (2021). Changing El Niño–Southern Oscillation in a warming climate.

- Nat. Rev. Earth Environ. 2, 628–644. <https://doi.org/10.1038/s43017-021-00199-z>.
12. Hsiang, S.M., Meng, K.C., and Cane, M.A. (2011). Civil conflicts are associated with the global climate. *Nature* 476, 438–441. <https://doi.org/10.1038/nature10311>.
13. Islam, F.S., Gault, A.G., Boothman, C., Polya, D.A., Charnock, J.M., Chatterjee, D., and Lloyd, J.R. (2004). Role of metal-reducing bacteria in arsenic release from Bengal delta sediments. *Nature* 430, 68–71. <https://doi.org/10.1038/nature02638>.
14. Cardil, A., Rodrigues, M., Tapia, M., Barbero, R., Ramírez, J., Stooft, C.R., Silva, C.A., Mohan, M., and de-Miguel, S. (2023). Climate teleconnections modulate global burned area. *Nat. Commun.* 14, 427. <https://doi.org/10.1038/s41467-023-36052-8>.
15. McPhaden, M.J., Zebiak, S.E., and Glantz, M.H. (2006). ENSO as an integrating concept in earth science. *Science* 314, 1740–1745. <https://doi.org/10.1126/science.1132588>.
16. Heino, M., Puma, M.J., Ward, P.J., Gerten, D., Heck, V., Siebert, S., and Kumm, M. (2018). Two-thirds of global cropland area impacted by climate oscillations. *Nat. Commun.* 9, 1257. <https://doi.org/10.1038/s41467-017-02071-5>.
17. Feng, P., Wang, B., Macadam, I., Taschetto, A.S., Abram, N.J., Luo, J.-J., King, A.D., Chen, Y., Li, Y., Liu, D.L., et al. (2022). Increasing dominance of Indian Ocean variability impacts Australian wheat yields. *Nat. Food* 3, 862–870. <https://doi.org/10.1038/s43016-022-00613-9>.
18. Jiang, J., and Zhou, T. (2023). Agricultural drought over water-scarce Central Asia aggravated by internal climate variability. *Nat. Geosci.* 16, 154–161. <https://doi.org/10.1038/s41561-022-01111-0>.
19. Iizumi, T., Luo, J.J., Challinor, A.J., Sakurai, G., Yokozawa, M., Sakuma, H., Brown, M.E., and Yamagata, T. (2014). Impacts of El Niño Southern Oscillation on the global yields of major crops. *Nat. Commun.* 5, 3712. <https://doi.org/10.1038/ncomms4712>.
20. Anderson, W., Baethgen, W., Capitanio, F., Ciais, P., Cook, B.I., Cunha, C.G.R.d., Goddard, L., Schaubert, B., Sonder, K., Podestà, G., et al. (2023). Climate variability and simultaneous breadbasket yield shocks as observed in long-term yield records. *Agric. For. Meteorol.* 337, 109321. <https://doi.org/10.1016/j.agrformet.2023.109321>.
21. Cao, J., Zhang, Z., Tao, F., Chen, Y., Luo, X., and Xie, J. (2023). Forecasting global crop yields based on El Niño Southern Oscillation early signals. *Agric. Syst.* 205, 103564. <https://doi.org/10.1016/j.agrformet.2023.103564>.
22. Collins, M., An, S.-I., Cai, W., Ganachaud, A., Guilyardi, E., Jin, F.-F., Jochum, M., Lengaigne, M., Power, S., Timmermann, A., et al. (2010). The impact of global warming on the tropical Pacific Ocean and El Niño. *Nat. Geosci.* 3, 391–397. <https://doi.org/10.1038/ngeo868>.
23. Wills, R.C.J., Dong, Y., Proistosescu, C., Armour, K.C., and Battisti, D.S. (2022). Systematic Climate Model Biases in the Large-Scale Patterns of Recent Sea-Surface Temperature and Sea-Level Pressure Change. *Geophys. Res. Lett.* 49, e2022GL100011. <https://doi.org/10.1029/2022gl100011>.
24. Tian, D., Asseng, S., Martinez, C.J., Misra, V., Cammarano, D., and Ortiz, B.V. (2015). Does decadal climate variation influence wheat and maize production in the southeast USA? *Agric. For. Meteorol.* 204, 1–9. <https://doi.org/10.1016/j.agrformet.2015.01.013>.
25. Fuentes-Franco, R., Docquier, D., Koenig, T., Zimmermann, K., and Giorgi, F. (2023). Winter heavy precipitation events over Northern Europe modulated by a weaker NAO variability by the end of the 21st century. *npj Clim. Atmos. Sci.* 6, 72. <https://doi.org/10.1038/s41612-023-00396-1>.
26. Cai, W., Ng, B., Wang, G., Santoso, A., Wu, L., and Yang, K. (2022). Increased ENSO sea surface temperature variability under four IPCC emission scenarios. *Nat. Clim. Chang.* 12, 228–231. <https://doi.org/10.1038/s41558-022-01282-z>.
27. Singh, J., Ashfaq, M., Skinner, C.B., Anderson, W.B., Mishra, V., and Singh, D. (2022). Enhanced risk of concurrent regional droughts with increased ENSO variability and warming. *Nat. Clim. Chang.* 12, 163–170. <https://doi.org/10.1038/s41558-021-01276-3>.
28. Sauer, I.J., Reese, R., Otto, C., Geiger, T., Willner, S.N., Guillod, B.P., Bresch, D.N., and Frieler, K. (2021). Climate signals in river flood damages emerge under sound regional disaggregation. *Nat. Commun.* 12, 2128. <https://doi.org/10.1038/s41467-021-22153-9>.
29. Emerton, R., Cloke, H.L., Stephens, E.M., Zsoter, E., Woolnough, S.J., and Pappenberger, F. (2017). Complex picture for likelihood of ENSO-driven flood hazard. *Nat. Commun.* 8, 14796. <https://doi.org/10.1038/ncomms14796>.
30. Janssens, C., Havlik, P., Krisztin, T., Baker, J., Frank, S., Hasegawa, T., Leclère, D., Ohrel, S., Ragnauth, S., Schmid, E., et al. (2020). Global hunger and climate change adaptation through international trade. *Nat. Clim. Chang.* 10, 829–835. <https://doi.org/10.1038/s41558-020-0847-4>.
31. Anderson, W.B., Seager, R., Baethgen, W., Cane, M., and You, L. (2019). Synchronous crop failures and climate-forced production variability. *Sci. Adv.* 5, eaaw1976.
32. Ng, C.H.J., Vecchi, G.A., Muñoz, Á.G., and Murakami, H. (2018). An asymmetric rainfall response to ENSO in East Asia. *Clim. Dyn.* 52, 2303–2318. <https://doi.org/10.1007/s00382-018-4253-9>.
33. Zhao, C., Liu, B., Piao, S., Wang, X., Lobell, D.B., Huang, Y., Huang, M., Yao, Y., Bassu, S., Ciais, P., et al. (2017). Temperature increase reduces global yields of major crops in four independent estimates. *Proc. Natl. Acad. Sci. USA* 114, 9326–9331. <https://doi.org/10.1073/pnas.1701762114>.
34. Jägermeyr, J., Müller, C., Ruane, A.C., Elliott, J., Balkovic, J., Castillo, O., Faye, B., Foster, I., Folberth, C., Franke, J.A., et al. (2021). Climate impacts on global agriculture emerge earlier in new generation of climate and crop models. *Nat. Food* 2, 873–885. <https://doi.org/10.1038/s43016-021-00400-y>.
35. Wang, X., Müller, C., Elliott, J., Mueller, N.D., Ciais, P., Jägermeyr, J., Gerber, J., Dumas, P., Wang, C., Yang, H., et al. (2021). Global irrigation contribution to wheat and maize yield. *Nat. Commun.* 12, 1235. <https://doi.org/10.1038/s41467-021-21498-5>.
36. Li, S., Zhuang, Y., Liu, H., Wang, Z., Zhang, F., Lv, M., Zhai, L., Fan, X., Niu, S., Chen, J., et al. (2023). Enhancing rice production sustainability and resilience via reactivating small water bodies for irrigation and drainage. *Nat. Commun.* 14, 3794. <https://doi.org/10.1038/s41467-023-39454-w>.
37. Li, L., Wang, B., Feng, P., Jägermeyr, J., Asseng, S., Müller, C., Macadam, I., Liu, D.L., Waters, C., Zhang, Y., et al. (2023). The optimization of model ensemble composition and size can enhance the robustness of crop yield projections. *Commun. Earth Environ.* 4, 362. <https://doi.org/10.1038/s43247-023-01016-9>.
38. Wang, G., Cai, W., Santoso, A., Abram, N., Ng, B., Yang, K., Geng, T., Doi, T., Du, Y., Izumo, T., et al. (2024). The Indian Ocean Dipole in a warming world. *Nat. Rev. Earth Environ.* 5, 588–604.
39. Schurer, A.P., Hegerl, G.C., Goosse, H., Bollasina, M.A., England, M.H., Smith, D.M., and Tett, S.F.B. (2023). Role of multi-decadal variability of the winter North Atlantic Oscillation on Northern Hemisphere climate. *Environ. Res. Lett.* 18, 044046.
40. Fredriksen, H.B., Berner, J., Subramanian, A.C., and Capotondi, A. (2020). How Does El Niño–Southern Oscillation Change Under Global Warming—A First Look at CMIP6. *Geophys. Res. Lett.* 47, e2020GL090640. <https://doi.org/10.1029/2020gl090640>.
41. Meehl, G.A., Senior, C.A., Eyring, V., Flato, G., Lamarque, J.-F., Stouffer, R.J., Taylor, K.E., and Schlund, M. (2020). Context for interpreting equilibrium climate sensitivity and transient climate response from the CMIP6 Earth system models. *Sci. Adv.* 6, eaaba1981.
42. Lauer, A., Eyring, V., Bellprat, O., Bock, L., Gier, B.K., Hunter, A., Lorenz, R., Pérez-Zanón, N., Righi, M., Schlund, M., et al. (2020). Earth System Model Evaluation Tool (ESMValTool) v2.0 – diagnostics for emergent constraints and future projections from Earth system models in CMIP. *Geosci. Model Dev. (GMD)* 13, 4205–4228. <https://doi.org/10.5194/gmd-13-4205-2020>.

43. Geng, X., Kug, J.-S., and Kosaka, Y. (2024). Future changes in the winter-time ENSO-NAO teleconnection under greenhouse warming. *npj Clim. Atmos. Sci.* 7, 81. <https://doi.org/10.1038/s41612-024-00627-z>.
44. Delworth, T.L., Zeng, F., Vecchi, G.A., Yang, X., Zhang, L., and Zhang, R. (2016). The North Atlantic Oscillation as a driver of rapid climate change in the Northern Hemisphere. *Nat. Geosci.* 9, 509–512. <https://doi.org/10.1038/ngeo2738>.
45. Scaife, A.A., and Smith, D. (2018). A signal-to-noise paradox in climate science. *npj Clim. Atmos. Sci.* 1, 28. <https://doi.org/10.1038/s41612-018-0038-4>.
46. Yao, Y., and Luo, D. (2018). An Asymmetric Spatiotemporal Connection between the Euro-Atlantic Blocking within the NAO Life Cycle and European Climates. *Adv. Atmos. Sci.* 35, 796–812. <https://doi.org/10.1007/s00376-017-7128-9>.
47. Castro-Díez, Y., Pozo-Vázquez, D., Rodrigo, F.S., and Esteban-Parra, M. J. (2002). NAO and winter temperature variability in southern Europe. *Geophys. Res. Lett.* 29, 1. <https://doi.org/10.1029/2001gl014042>.
48. Zhang, Y., Li, C., Chiew, F.H.S., Post, D.A., Zhang, X., Ma, N., Tian, J., Kong, D., Leung, L.R., Yu, Q., et al. (2023). Southern Hemisphere dominates recent decline in global water availability. *Science* 382, 579–584. <https://doi.org/10.1126/science.adh0716>.
49. Cai, W., Santoso, A., Wang, G., Weller, E., Wu, L., Ashok, K., Masumoto, Y., and Yamagata, T. (2014). Increased frequency of extreme Indian Ocean Dipole events due to greenhouse warming. *Nature* 510, 254–258. <https://doi.org/10.1038/nature13327>.
50. Cai, W., Cowan, T., and Raupach, M. (2009). Positive Indian Ocean Dipole events precondition southeast Australia bushfires. *Geophys. Res. Lett.* 36, L19710. <https://doi.org/10.1029/2009gl039902>.
51. Wang, J., Wang, M., Kim, J.S., Joiner, J., Zeng, N., Jiang, F., Wang, H., He, W., Wu, M., Chen, T., et al. (2021). Modulation of Land Photosynthesis by the Indian Ocean Dipole: Satellite-Based Observations and CMIP6 Future Projections. *Earths Future* 9, e2020EF001942. <https://doi.org/10.1029/2020ef001942>.
52. Heino, M., Guillaume, J.H.A., Müller, C., Izumi, T., and Kumm, M. (2020). A multi-model analysis of teleconnected crop yield variability in a range of cropping systems. *Earth Syst. Dyn.* 11, 113–128. <https://doi.org/10.5194/esd-11-113-2020>.
53. Le, T., Ha, K.J., and Bae, D.H. (2021). Increasing Causal Effects of El Niño–Southern Oscillation on the Future Carbon Cycle of Terrestrial Ecosystems. *Geophys. Res. Lett.* 48, e2021GL095804. <https://doi.org/10.1029/2021gl095804>.
54. Le, T., and Bae, D.H. (2022). Causal Impacts of El Niño–Southern Oscillation on Global Soil Moisture Over the Period 2015–2100. *Earths Future* 10, e2021EF002522. <https://doi.org/10.1029/2021ef002522>.
55. Cai, W., Borlace, S., Lengaigne, M., van Rensch, P., Collins, M., Vecchi, G., Timmermann, A., Santoso, A., McPhaden, M.J., Wu, L., et al. (2014). Increasing frequency of extreme El Niño events due to greenhouse warming. *Nat. Clim. Chang.* 4, 111–116. <https://doi.org/10.1038/nclimate2100>.
56. Wang, G., Cai, W., Gan, B., Wu, L., Santoso, A., Lin, X., Chen, Z., and McPhaden, M.J. (2017). Continued increase of extreme El Niño frequency long after 1.5 °C warming stabilization. *Nat. Clim. Chang.* 7, 568–572. <https://doi.org/10.1038/nclimate3351>.
57. Meyers, G., McIntosh, P., Pigot, L., and Pook, M. (2007). The Years of El Niño, La Niña, and Interactions with the Tropical Indian Ocean. *J. Clim.* 20, 2872–2880. <https://doi.org/10.1175/jcli4152.1>.
58. Izumo, T., Vialard, J., Lengaigne, M., de Boyer Montegut, C., Behera, S. K., Luo, J.-J., Cravatte, S., Masson, S., and Yamagata, T. (2010). Influence of the state of the Indian Ocean Dipole on the following year's El Niño. *Nat. Geosci.* 3, 168–172. <https://doi.org/10.1038/ngeo760>.
59. Ham, Y.-G., Choi, J.-Y., and Kug, J.-S. (2016). The weakening of the ENSO–Indian Ocean Dipole (IOD) coupling strength in recent decades. *Clim. Dyn.* 49, 249–261. <https://doi.org/10.1007/s00382-016-3339-5>.
60. Wang, J., Liu, Z., Zeng, N., Jiang, F., Wang, H., and Ju, W. (2020). Spaceborne detection of XCO₂ enhancement induced by Australian mega-bushfires. *Environ. Res. Lett.* 15, 124069. <https://doi.org/10.1088/1748-9326/abc846>.
61. Phillips, N., and Nogrady, B. (2020). The race to decipher how climate change influenced Australia's record fires. *Nature* 577, 610–612.
62. Stephenson, D.B., Pavan, V., Collins, M., Junge, M.M., and Quadrelli, R. (2006). North Atlantic Oscillation response to transient greenhouse gas forcing and the impact on European winter climate: a CMIP2 multi-model assessment. *Clim. Dyn.* 27, 401–420. <https://doi.org/10.1007/s00382-006-0140-x>.
63. Sippel, S., Reichstein, M., Ma, X., Mahecha, M.D., Lange, H., Flach, M., and Frank, D. (2018). Drought, Heat, and the Carbon Cycle: a Review. *Curr. Clim. Change Rep.* 4, 266–286. <https://doi.org/10.1007/s40641-018-0103-4>.
64. McKenna, C.M., and Maycock, A.C. (2021). Sources of Uncertainty in Multimodel Large Ensemble Projections of the Winter North Atlantic Oscillation. *Geophys. Res. Lett.* 48, e2021GL093258. <https://doi.org/10.1029/2021gl093258>.
65. Wang, B., Sun, W., Jin, C., Luo, X., Yang, Y.-M., Li, T., Xiang, B., McPhaden, M.J., Cane, M.A., Jin, F., et al. (2023). Understanding the recent increase in multiyear La Niñas. *Nat. Clim. Chang.* 13, 1075–1081. <https://doi.org/10.1038/s41558-023-01801-6>.
66. Geng, T., Jia, F., Cai, W., Wu, L., Gan, B., Jing, Z., Li, S., and McPhaden, M.J. (2023). Increased occurrences of consecutive La Niña events under global warming. *Nature* 619, 774–781. <https://doi.org/10.1038/s41586-023-06236-9>.
67. Guimarães, Y.C., Londe, L., Massi, K., Marengo, J., Nobre, C.A., Assireu, A.T., Bortolozzo, C.A., Simões, S.J., Tomasella, J., and de Moraes, O.L.L. (2024). Unprecedented Flooding in Porto Alegre Metropolitan Region (Southern 2 Brazil) in May 2024: Causes, Risks, and Impacts.
68. Hoyos, N., Escobar, J., Restrepo, J.C., Arango, A.M., and Ortiz, J.C. (2013). Impact of the 2010–2011 La Niña phenomenon in Colombia, South America: The human toll of an extreme weather event. *Appl. Geogr.* 39, 16–25. <https://doi.org/10.1016/j.apgeog.2012.11.018>.
69. Han, J., Zhang, Z., Xu, J., Chen, Y., Jägermeyr, J., Cao, J., Luo, Y., Cheng, F., Zhuang, H., Wu, H., et al. (2024). Threat of low-frequency high-intensity floods to global cropland and crop yields. *Nat. Sustain.* 7, 994–1006.
70. Fu, J., Jian, Y., Wang, X., Li, L., Ciais, P., Zscheischler, J., Wang, Y., Tang, Y., Müller, C., Webber, H., et al. (2023). Extreme rainfall reduces one-twelfth of China's rice yield over the last two decades. *Nat. Food* 4, 416–426. <https://doi.org/10.1038/s43016-023-00753-6>.
71. Li, Y., Guan, K., Schnitkey, G.D., DeLucia, E., and Peng, B. (2019). Excessive rainfall leads to maize yield loss of a comparable magnitude to extreme drought in the United States. *Glob. Chang. Biol.* 25, 2325–2337. <https://doi.org/10.1111/gcb.14628>.
72. Xiong, W., Asseng, S., Hoogenboom, G., Hernandez-Ochoa, I., Robertson, R., Sonder, K., Pequeno, D., Reynolds, M., and Gerard, B. (2019). Different uncertainty distribution between high and low latitudes in modelling warming impacts on wheat. *Nat. Food* 1, 63–69. <https://doi.org/10.1038/s43016-019-0004-2>.
73. Wang, B., Feng, P., Liu, D.L., O'Leary, G.J., Macadam, I., Waters, C., Asseng, S., Cowie, A., Jiang, T., Xiao, D., et al. (2020). Sources of uncertainty for wheat yield projections under future climate are site-specific. *Nat. Food* 1, 720–728. <https://doi.org/10.1038/s43016-020-00181-w>.
74. Asseng, S., Ewert, F., Rosenzweig, C., Jones, J.W., Hatfield, J.L., Ruane, A.C., Boote, K.J., Thorburn, P.J., Rötter, R.P., Cammarano, D., et al. (2013). Uncertainty in simulating wheat yields under climate change. *Nat. Clim. Chang.* 3, 827–832.
75. Heinicke, S., Frieler, K., Jägermeyr, J., and Mengel, M. (2022). Global gridded crop models underestimate yield responses to droughts and heatwaves. *Environ. Res. Lett.* 17, 044026. <https://doi.org/10.1088/1748-9326/ac592e>.

76. Wang, X., Zhao, C., Müller, C., Wang, C., Ciais, P., Janssens, I., Peñuelas, J., Asseng, S., Li, T., Elliott, J., et al. (2020). Emergent constraint on crop yield response to warmer temperature from field experiments. *Nat. Sustain.* 3, 908–916. <https://doi.org/10.1038/s41893-020-0569-7>.
77. Li, L., Zhang, Y., Wang, B., Feng, P., He, Q., Shi, Y., Liu, K., Harrison, M. T., Liu, D.L., Yao, N., et al. (2023). Integrating machine learning and environmental variables to constrain uncertainty in crop yield change projections under climate change. *Eur. J. Agron.* 149, 126917. <https://doi.org/10.1016/j.eja.2023.126917>.
78. Müller, C., Franke, J., Jägermeyr, J., Ruane, A.C., Elliott, J., Moyer, E., Heinke, J., Falloon, P.D., Folberth, C., Francois, L., et al. (2021). Exploring uncertainties in global crop yield projections in a large ensemble of crop models and CMIP5 and CMIP6 climate scenarios. *Environ. Res. Lett.* 16, 034040. <https://doi.org/10.1088/1748-9326/abd8fc>.
79. Lee, J., Planton, Y.Y., Gleckler, P.J., Sperber, K.R., Guilyardi, E., Wittenberg, A.T., McPhaden, M.J., and Pallotta, G. (2021). Robust Evaluation of ENSO in Climate Models: How Many Ensemble Members Are Needed? *Geophys. Res. Lett.* 48, e2021GL095041. <https://doi.org/10.1029/2021gl095041>.
80. Wang, K., Wang, X., Piao, S., Chevallier, F., Mao, J., Shi, X., Huntingford, C., Bastos, A., Ciais, P., Xu, H., et al. (2021). Unusual characteristics of the carbon cycle during the 2015–2016 El Niño. *Glob. Chang. Biol.* 27, 3798–3809. <https://doi.org/10.1111/gcb.15669>.
81. Anttila-Hughes, J.K., Jina, A.S., and McCord, G.C. (2021). ENSO impacts child undernutrition in the global tropics. *Nat. Commun.* 12, 5785. <https://doi.org/10.1038/s41467-021-26048-7>.
82. Liu, Y., Cai, W., Lin, X., Li, Z., and Zhang, Y. (2023). Nonlinear El Niño impacts on the global economy under climate change. *Nat. Commun.* 14, 5887. <https://doi.org/10.1038/s41467-023-41551-9>.
83. Davis, K.F., Downs, S., and Gephart, J.A. (2021). Towards food supply chain resilience to environmental shocks. *Nat. Food* 2, 54–65. <https://doi.org/10.1038/s43016-020-00196-3>.
84. Gomez, M., Mejia, A., Ruddell, B.L., and Rushforth, R.R. (2021). Supply chain diversity buffers cities against food shocks. *Nature* 595, 250–254. <https://doi.org/10.1038/s41586-021-03621-0>.
85. Ribeiro, J.M.P., Berchin, I.I., da Silva Neiva, S., Soares, T., de Albuquerque Junior, C.L., Degga, A.B., de Amorim, W.S., Barbosa, S. B., Secchi, L., and de Andrade Guerra, J.B.S.O. (2020). Food stability model: A framework to support decision-making in a context of climate change. *Sustain. Dev.* 29, 13–24. <https://doi.org/10.1002/sd.2128>.
86. Brander, M., Bernauer, T., and Huss, M. (2023). Trade policy announcements can increase price volatility in global food commodity markets. *Nat. Food* 4, 331–340. <https://doi.org/10.1038/s43016-023-00729-6>.
87. Bren d'Amour, C., Wenz, L., Kalkuhl, M., Christoph Steckel, J., and Creutzig, F. (2016). Teleconnected food supply shocks. *Environ. Res. Lett.* 11, 035007. <https://doi.org/10.1088/1748-9326/11/3/035007>.
88. Chen, B., and Villoria, N.B. (2019). Climate shocks, food price stability and international trade: evidence from 76 maize markets in 27 net-importing countries. *Environ. Res. Lett.* 14, 014007. <https://doi.org/10.1088/1748-9326/aaf07f>.
89. Gilbert, C.L., and Morgan, C.W. (2010). Food price volatility. *Philos. Trans. R. Soc. Lond. B Biol. Sci.* 365, 3023–3034. <https://doi.org/10.1098/rstb.2010.0139>.
90. Wang, B., Jägermeyr, J., O'Leary, G.J., Wallach, D., Ruane, A.C., Feng, P., Li, L., Liu, L., Waters, C., Yu, Q., et al. (2024). Pathways to identify and reduce uncertainties in agricultural climate impact assessments. *Nat. Food* 5, 550–556. <https://doi.org/10.1038/s43016-024-01014-w>.
91. Maher, N., Matei, D., Milinski, S., and Marotzke, J. (2018). ENSO Change in Climate Projections: Forced Response or Internal Variability? *Geophys. Res. Lett.* 45, 11–390. <https://doi.org/10.1029/2018gl079764>.
92. Cai, W., Ng, B., Geng, T., Wu, L., Santoso, A., and McPhaden, M.J. (2020). Butterfly effect and a self-modulating El Niño response to global warming. *Nature* 585, 68–73. <https://doi.org/10.1038/s41586-020-2641-x>.
93. Cai, W., Ng, B., Geng, T., Jia, F., Wu, L., Wang, G., Liu, Y., Gan, B., Yang, K., Santoso, A., et al. (2023). Anthropogenic impacts on twentieth-century ENSO variability changes. *Nat. Rev. Earth Environ.* 4, 407–418. <https://doi.org/10.1038/s43017-023-00427-8>.
94. Tang, T., Luo, J.J., Peng, K., Qi, L., and Tang, S. (2021). Over-projected Pacific warming and extreme El Niño frequency due to CMIP5 common biases. *Natl. Sci. Rev.* 8, nwab056. <https://doi.org/10.1093/nsr/nwab056>.
95. Minoli, S., Jägermeyr, J., Asseng, S., Urfels, A., and Müller, C. (2022). Global crop yields can be lifted by timely adaptation of growing periods to climate change. *Nat. Commun.* 13, 7079. <https://doi.org/10.1038/s41467-022-34411-5>.
96. McCullough, E.B., Quinn, J.D., and Simons, A.M. (2022). Profitability of climate-smart soil fertility investment varies widely across sub-Saharan Africa. *Nat. Food* 3, 275–285. <https://doi.org/10.1038/s43016-022-00493-z>.
97. Baldos, U.L.C., and Hertel, T.W. (2015). The role of international trade in managing food security risks from climate change. *Food Secur.* 7, 275–290. <https://doi.org/10.1007/s12571-015-0435-z>.
98. Friel, S., Schram, A., and Townsend, B. (2020). The nexus between international trade, food systems, malnutrition and climate change. *Nat. Food* 1, 51–58. <https://doi.org/10.1038/s43016-019-0014-0>.
99. Porfirio, L.L., Newth, D., Finnigan, J.J., and Cai, Y. (2018). Economic shifts in agricultural production and trade due to climate change. *Palgrave Commun.* 4, 111. <https://doi.org/10.1057/s41599-018-0164-y>.
100. Portmann, F.T., Siebert, S., and Döll, P. (2010). MIRCA2000—Global monthly irrigated and rainfed crop areas around the year 2000: A new high-resolution data set for agricultural and hydrological modeling. *Glob. Biogeochem. Cycles* 24, GB1011. <https://doi.org/10.1029/2008gb003435>.
101. Schillerberg, T.A., Tian, D., and Miao, R. (2019). Spatiotemporal patterns of maize and winter wheat yields in the United States: Predictability and impact from climate oscillations. *Agric. For. Meteorol.* 275, 208–222. <https://doi.org/10.1016/j.agrformet.2019.05.019>.
102. Nouri, N., Devineni, N., Were, V., and Khanbilvardi, R. (2021). Explaining the trends and variability in the United States tornado records using climate teleconnections and shifts in observational practices. *Sci. Rep.* 11, 1741. <https://doi.org/10.1038/s41598-021-81143-5>.
103. Rayner, N.A., Parker, D.E., Horton, E.B., Folland, C.K., Alexander, L.V., Rowell, D.P., Kent, E.C., and Kaplan, A. (2003). Global analyses of sea surface temperature, sea ice, and night marine air temperature since the late nineteenth century. *J. Geophys. Res.* 108, 4407. <https://doi.org/10.1029/2002jd002670>.
104. McPhaden, M.J., Santoso, A., and Cai, W. (2020). *El Niño Southern Oscillation in a Changing Climate* (John Wiley & Sons).
105. Wang, B., Feng, P., Waters, C., Cleverly, J., Liu, D.L., and Yu, Q. (2020). Quantifying the impacts of pre-occurred ENSO signals on wheat yield variation using machine learning in Australia. *Agric. For. Meteorol.* 291, 108043. <https://doi.org/10.1016/j.agrformet.2020.108043>.
106. Shuai, J., Zhang, Z., Tao, F., and Shi, P. (2016). How ENSO affects maize yields in China: understanding the impact mechanisms using a process-based crop model. *Int. J. Climatol.* 36, 424–438. <https://doi.org/10.1002/joc.4360>.
107. Saji, N., and Yamagata, T. (2003). Possible impacts of Indian Ocean dipole mode events on global climate. *Clim. Res.* 25, 151–169.
108. Saji, N.H., Goswami, B.N., Vinayachandran, P.N., and Yamagata, T. (1999). A dipole mode in the tropical Indian Ocean. *Nature* 401, 360–363.
109. Bastos, A., Janssens, I.A., Gouveia, C.M., Trigo, R.M., Ciais, P., Chevallier, F., Peñuelas, J., Rödenbeck, C., Piao, S., Friedlingstein, P., and Running, S.W. (2016). European land CO₂ sink influenced by NAO

- and East-Atlantic Pattern coupling. *Nat. Commun.* 7, 10315. <https://doi.org/10.1038/ncomms10315>.
110. Tian, H., Yang, J., Xu, R., Lu, C., Canadell, J.G., Davidson, E.A., Jackson, R.B., Arndt, A., Chang, J., Ciais, P., et al. (2019). Global soil nitrous oxide emissions since the preindustrial era estimated by an ensemble of terrestrial biosphere models: Magnitude, attribution, and uncertainty. *Glob. Chang. Biol.* 25, 640–659. <https://doi.org/10.1111/gcb.14514>.
111. Klueter, A., Crandall, J.B., Archer, F.I., Teece, M.A., and Coffroth, M.A. (2015). Taxonomic and environmental variation of metabolite profiles in marine dinoflagellates of the genus symbiodinium. *Metabolites* 5, 74–99. <https://doi.org/10.3390/metabo5010074>.
112. Stocker, T.F., Qin, D., Plattner, G.-K., Tignor, M., Allen, S.K., Boschung, J., Nauels, A., Xia, Y., Bex, V., and Midgley, P.M. (2013). *The Physical Science Basis. Contribution of Working Group I to the Fifth Assessment Report of the Intergovernmental Panel on Climate Change* (Cambridge University Press).
113. Friedman, J.H. (2001). Greedy function approximation: a gradient boosting machine. *Ann. Stat.* 29, 1189–1232.